Protective effect of newly synthesized and characterized charge transfer (CT) complex against arecoline induced carcinogenicity in third-instar larvae of transgenic *Drosophila melanogaster (hsp70-lacZ) Bg⁹*: Experimental and theoretical mechanistic insights

Sonam Shakya[a], Ishaat M. Khan[a,*], Barkha Shakya[b], Yasir Hasan Siddique[b], Himanshi Varshney[b], Smita Jyoti[b]

[a]*Department of Chemistry, Aligarh Muslim University, Aligarh 202002, India*
Department of Zoology, Aligarh Muslim University, Aligarh 202002, India

ENERGY COMPONENTS OF CL

Wavefunction normalization = 1.0000000000

One electron energy = -4833.6816174153

Two electron energy = 2057.6396817447

Nuclear repulsion energy = 1650.5026906198

Total Energy = -1146.5392450508

Electron-electron potential energy = 2057.6396817447

Nucleus-electron potential energy = -5950.4545023506

Nucleus-nucleus potential energy = 1650.5026906198

Total potential energy = -2242.3121299861

Total kinetic energy = 1116.7728849353

Virial ratio (V/T) = 2.0078497251

FTIR study for PYZ, TNP and CL

FTIR spectrum of $[(PYZH)^{+}(TNP)^{-}]$ was studied in comparison with the spectra of respective reactants (PYZ and TNP), represented in Fig. S1. On reviewing the spectra of PYZ, TNP, and **CL**, we observed C-N stretching vibrations at 1465 and 1395 cm^{-1} for free PYZ while they were appeared at 1473 and 1399 cm^{-1} in the spectrum of **CL**. These bands were shifted to the high frequency region in **CL** spectrum due to the transfer of electron density from the donor to the acceptor, which was a good agreement for the formation of the resulting CT complex.[1] Similarly, O-H stretching vibrations appeared at 3431 cm^{-1} in TNP, while the same was found at 3427 cm^{-1} in **CL** FTIR. A new band at 3218 cm^{-1} has appeared, indicating N^{+}—H---O^{-} stretching vibration, which suggests H-bonding between TNP and PYZ. Most of the bands of **CL** were observed to be shifted to higher frequencies to PYZ while lower frequencies to TNP.[2] Symmetric and asymmetric NO_2 stretching vibrations were at 1337 and 1528 cm^{-1} in TNP, but appeared at 1365 and 1542 cm^{-1} in **CL** FTIR. The C—H aromatic stretching band of TNP and PYZ were appeared at 3106 and 3121 cm^{-1}, respectively, while at 3139 cm^{-1} in **CL** spectrum. This change in the frequencies is because of the transfer of an electron from TNP to PYZ (N atom); this results in increased electron density in the nitro groups.[3]

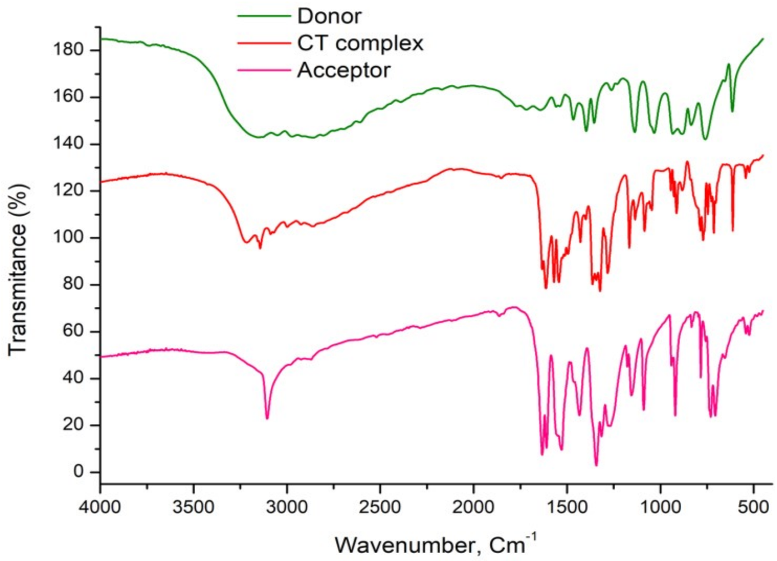

Fig. S1. FTIR spectra of PYZ, TNP, and charge transfer complex (**CL**).

P-XRD pattern

The P-XRD pattern was recorded for the designed material **CL**. P-XRD technique is used to understand the bulk purity of the **CL** as well as its composition. As shown in Fig. S4, the simulated P-XRD pattern of the single crystal obtained the SC-XRD data and the powder X-ray diffraction patterns of synthesized **CL** are in good agreement. This confirms the bulk purity of the **CL**. Sharp and well-defined Bragg's peak in the PXRD pattern is observed at diffraction angle 2θ at which reveals that the **CL** is semi-crystalline in nature.

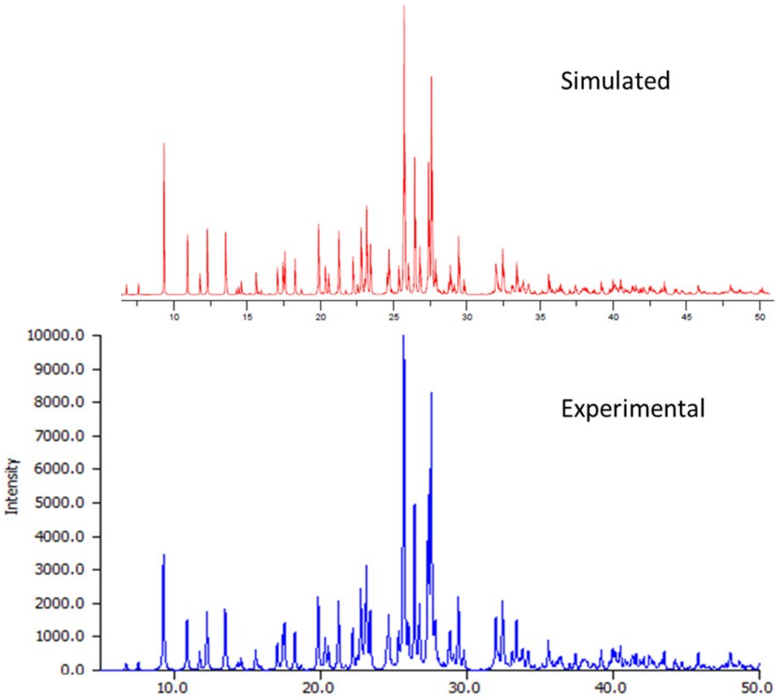

Fig. S2. Powder XRD patterns of **CL**- experimental (bottom) and simulated (top).

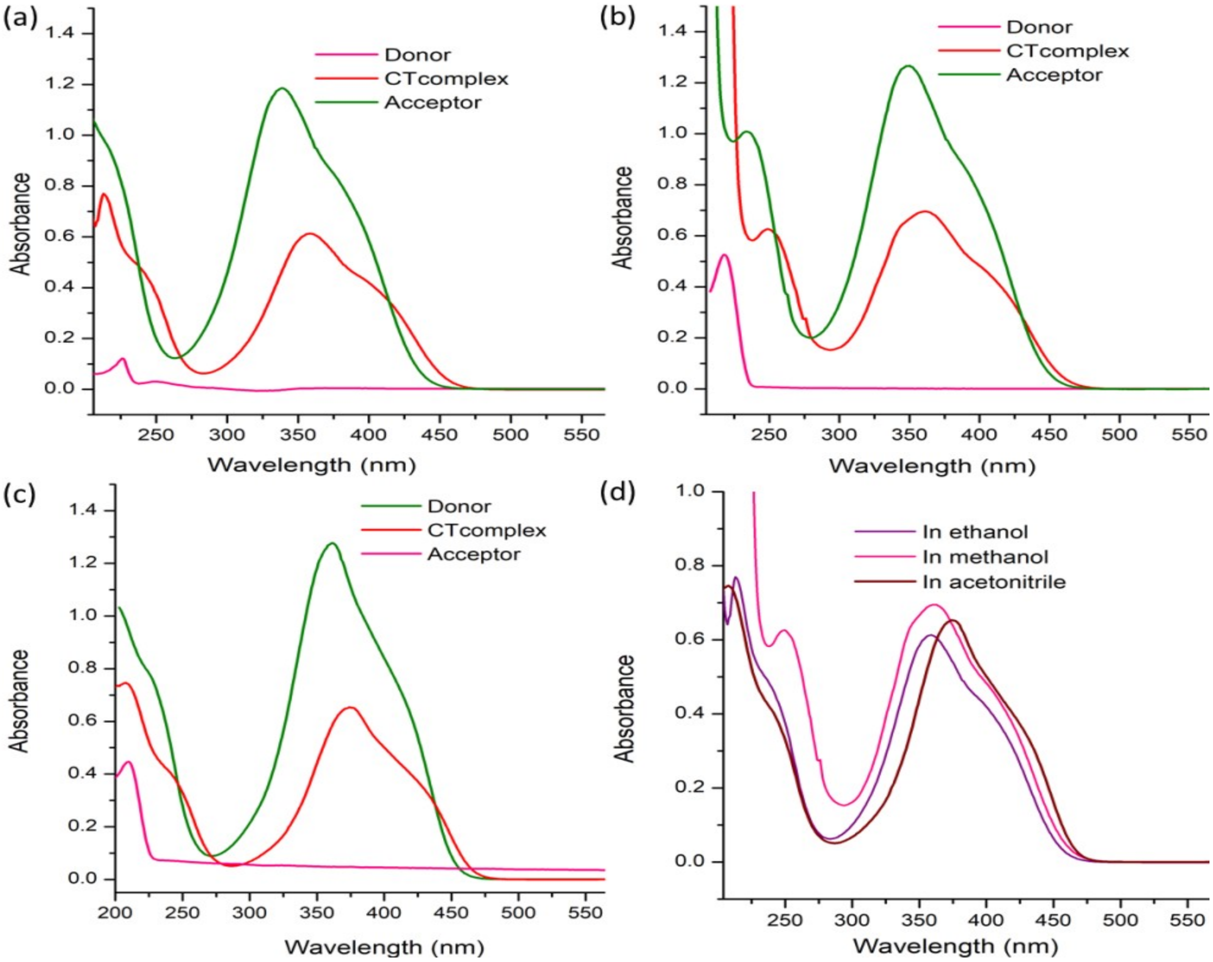

Fig. S3. Electronic absorption spectra of donor (PYZ), donor-acceptor CT complex (**CL**), and acceptor (TNP) (a) ethanol, (b) methanol, (c) acetonitrile, and (d) Comparative electronic absorption spectra of **CL** in ethanol, methanol, and acetonitrile.

Table S1. Absorption data for spectrophotometric determination of formation constant (K_{CT}) and molar extinction coefficient (ε_{CT}) of **CL** at room temperature.

Concentration of donor (M)	**Concentration of acceptor (M)**	**Absorbance at λ_{CT} (nm)**	**Formation constant (K_{CT}) l mol^{-1}**	**Molar extinction coefficient (ε_{CT}) l cm^{-1} mol^{-1}**
Ethanol		At 358 nm		
1.5×10^{-4}	1.0×10^{-4}	0.6153	3.32×10^{4}	4.49×10^{3}
2.0×10^{-4}		0.6299		
2.5×10^{-4}		0.7458		
3.0 × 10-4		0.7499		
Methanol		At 361 nm	3.01×10^{4}	4.87×10^{3}
1.5×10^{-4}	1.0×10^{-4}	0.6971		
2.0×10^{-4}		0.7416		
2.5×10^{-4}		0.8601		
3.0 × 10-4		0.9924		
Acetonitrile		At 374 nm	1.71×10^{4}	5.54×10^{3}
1.5×10^{-4}	1.0×10^{-4}	0.6556		
2.0×10^{-4}		0.7891		
2.5×10^{-4}		0.8657		
3.0 × 10-4		0.9911		

Table S2. Gaussian curve analysis for **CL** of PYZ with TNP in different solvents.

Solvent	**Area of the curve (*A*)**	**Width of the curve (*w*)**	**Centre of the curve (x_c)**	**y_0**
Ethanol	66.47 ± 3.04	100.49 ± 2.69	369.75 ± 0.39	0.05 ± 0.001
Methanol	80.55 ± 4.60	106.27 ± 3.29	368.60 ± 0.42	0.04 ± 0.002
Acetonitrile	66.48 ± 2.63	96.62 ± 2.34	383.17 ± 0.37	0.03 ± 0.001

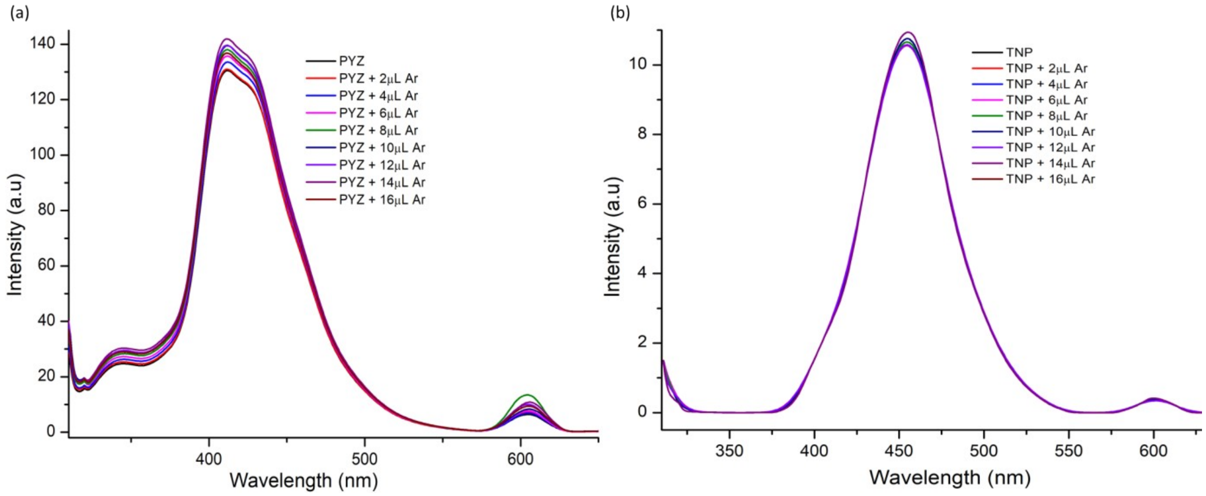

Fig. S4. The change in fluorescence intensity of (a) PYZ and (b) TNP on gradual addition of arecoline.

Table S3. Bond Lengths for **CL**.

Atoms 1—2	**Length 1—2 [Å]**	**Atoms 1—2**	**Length 1—2 [Å]**
O1—N1	1.228(3)	C18—H18	0.9500
O2—N1	1.231(3)	O8—N6	1.227(3)
O3—N2	1.229(3)	O9—N6	1.234(3)
O4—N2	1.229(3)	O10—N7	1.232(3)
O5—N3	1.221(3)	O11—N7	1.231(3)
O6—N3	1.233(3)	O12—N8	1.227(3)
O7—C2	1.256(3)	O13—N8	1.228(3)
O15—H15a	0.8500	O14—C11	1.258(3)
O15—H15b	0.84(4)	N6—C12	1.458(3)
N1—C1	1.455(3)	N7—C14	1.451(3)
N2—C5	1.449(3)	N8—C10	1.464(3)
N3—C3	1.458(3)	C10—C11	1.450(4)
N9—N10	1.342(3)	C10—C15	1.377(4)
N9—C16	1.331(3)	C11—C12	1.450(4)
N9—H9a	0.89(3)	C12—C13	1.376(4)
N10—C18	1.329(3)	C13—H13	0.9500
N10—H10	0.86(3)	C13—C14	1.383(4)
C1—C2	1.462(3)	C14—C15	1.384(4)
C1—C6	1.372(4)	C15—H15	0.9500
C2—C3	1.446(4)	N4—N5	1.343(3)
C3—C4	1.379(4)	N4—C7	1.331(4)
C4—H4	0.9500	N4—H4a	0.88(3)
C4—C5	1.372(4)	N5—C9	1.328(3)
C5—C6	1.391(4)	N5—H5	0.88(3)
C6—H6	0.9500	C7—H7	0.9500
C16—H16	0.9500	C7—C8	1.377(4)

C16—C17	1.379(4)	C8—H8	0.9500
C17—H17	0.9500	C8—C9	1.378(4)
C17—C18	1.377(4)	C9—H9	0.9500

Table S4. Hydrogen Atom Coordinates (Å×10^4) and Isotropic Displacement Parameters (Å^2×10^3) for **CL**.

Atom	***x***	***y***	***z***	**U(eq)**
H15a	9480(40)	7610(20)	7886(18)	24.5(7)
H4	8359(3)	5362(2)	11662(2)	15.8(7)
H6	5974(3)	3999(2)	8756(2)	16.2(7)
H16	12942(4)	11143(2)	8814(2)	20.8(7)
H17	13904(4)	11422(2)	10725(2)	18.8(7)
H18	12641(4)	9704(2)	11286(2)	19.6(7)
H10	10980(40)	8530(30)	9710(20)	23(9)
H15b	8920(50)	8070(30)	7020(30)	38(11)
H9a	11180(50)	9290(30)	8330(30)	36(10)
H13	3563(4)	8388(2)	2807(2)	17.4(7)
H15	2285(4)	9249(2)	5573(2)	17.9(7)
H7	13566(4)	5782(2)	6583(2)	23.8(8)
H8	13352(4)	5137(2)	4710(2)	24.3(8)
H9	10682(4)	6012(2)	3799(2)	20.2(7)
H5	9420(40)	7100(30)	5160(20)	25(9)
H4a	11040(40)	7030(30)	6690(20)	17(8)

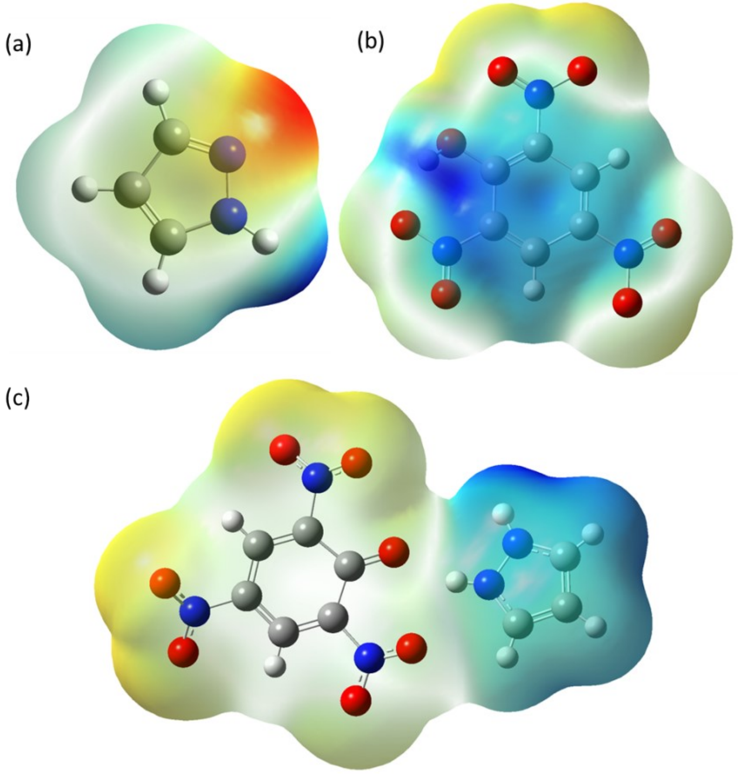

Fig. S5. MEP surface map of (a) PYZ, (b) TNP, and (c) **CL**, showing difference in color.

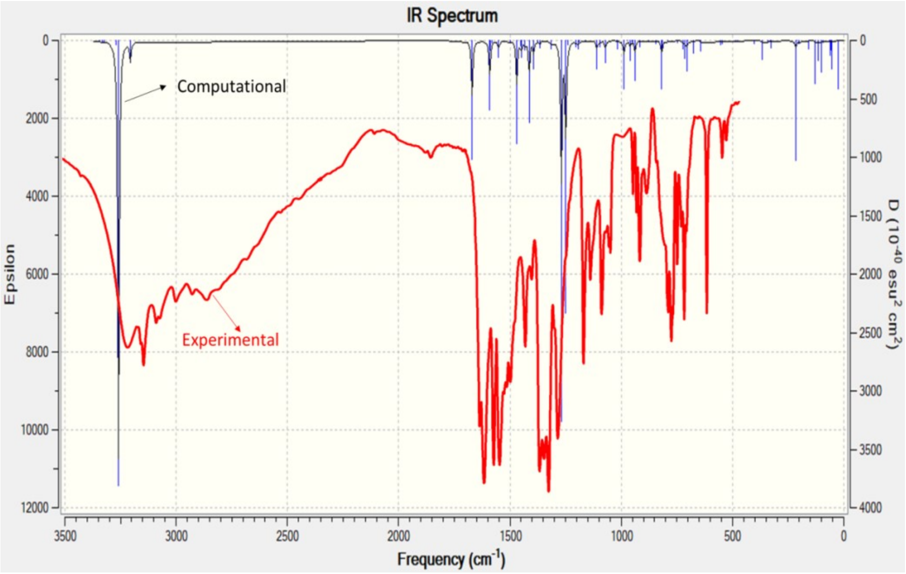

Fig. S6. Computational (black) and experimental (red) FTIR spectrum of **CL**.

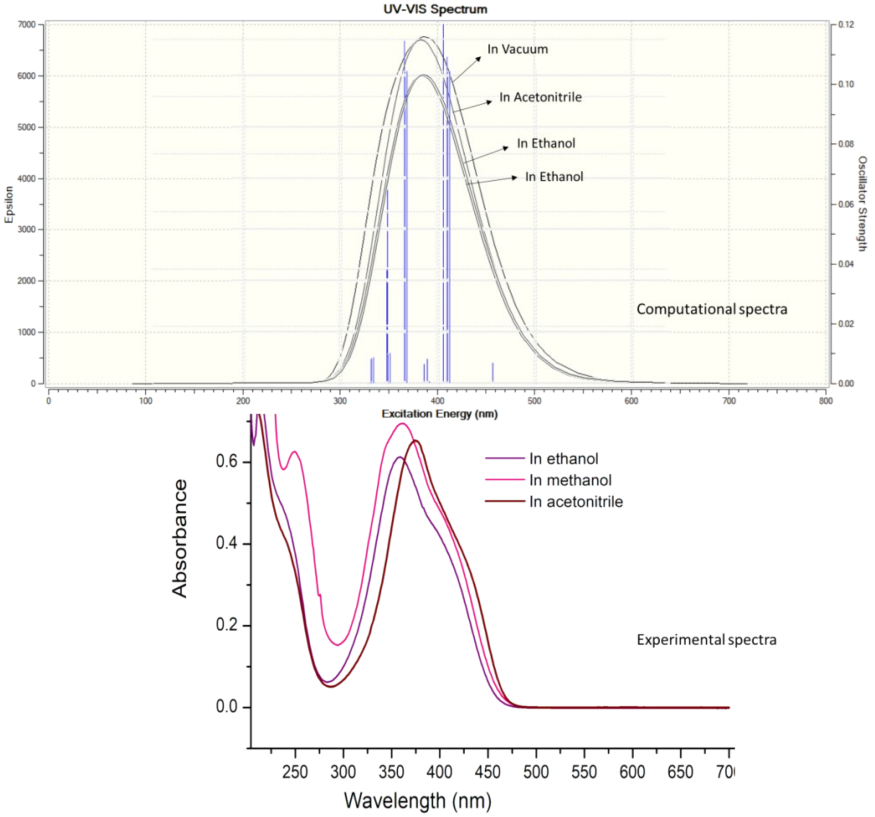

Fig. S7. Computational (TD-DFT) UV-vis spectrum (top) and experimental UV-vis spectrum in different solvents (bottom) of **CL**.

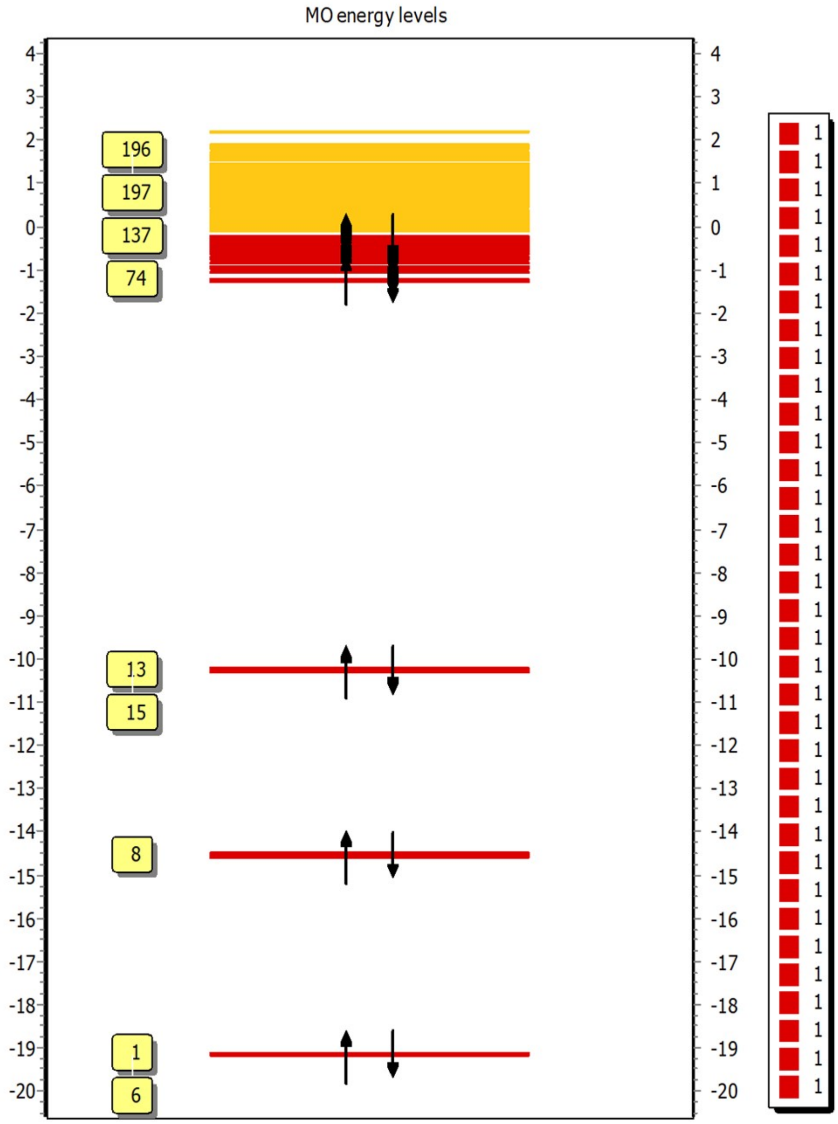

Fig. S8. MO energy level diagram of **CL**.

Table S5. Molecular orbital energies for **CL** (HOMO = 1 -76 and LUMO = 77-108).

MO NO.	**Energy (a.u)**	**MO NO.**	**Energy**	**MO NO.**	**Energy (a.u)**
1	-19.1833	37	-0.73485	73	-0.27912
2	-19.1796	38	-0.72934	74	-0.27021
3	-19.1662	39	-0.72163	75	-0.24901
4	-19.1656	40	-0.68804	76	-0.2257
5	-19.1624	41	-0.61986	77	-0.10594
6	-19.1621	42	-0.59559	78	-0.09516
7	-19.1213	43	-0.59101	79	-0.07346
8	-14.5683	44	-0.5805	80	-0.06554
9	-14.5516	45	-0.57157	81	-0.02389
1	-14.5495	46	-0.55371	82	0.00723
11	-14.5173	47	-0.55329	83	0.02196
12	-14.4986	48	-0.55097	84	0.0448
13	-10.3211	49	-0.5436	85	0.08037
14	-10.3105	50	-0.53897	86	0.10094
15	-10.2867	51	-0.52657	87	0.10531
16	-10.2626	52	-0.52225	88	0.11843
17	-10.2462	53	-0.5197	89	0.14013
18	-10.2416	54	-0.50941	90	0.14604
19	-10.2415	55	-0.50482	91	0.15208
20	-10.2146	56	-0.49141	92	0.1654
21	-10.2136	57	-0.48062	93	0.17667
22	-1.25843	58	-0.46981	94	0.19618
23	-1.24063	59	-0.43101	95	0.21096
24	-1.24049	60	-0.42388	96	0.22737
25	-1.20843	61	-0.4149	97	0.23825
26	-1.0767	62	-0.38916	98	0.26125
27	-1.06113	63	-0.36498	99	0.26861
28	-1.05925	64	-0.35257	100	0.27547
29	-1.03421	65	-0.32169	101	0.28618
30	-0.98036	66	-0.31403	102	0.30363
31	-0.9289	67	-0.30448	103	0.31228
32	-0.90785	68	-0.30093	104	0.31764
33	-0.84339	69	-0.29656	105	0.33249
34	-0.82429	70	-0.2931	106	0.34419
35	-0.76434	71	-0.29051	107	0.35197
36	-0.75331	72	-0.28525	108	0.36821

Table S6. Coordinates of TNP molecule obtained from DFT calculations.

Center Number	Atom	Atomic Number	Coordinates (Angstroms)		
			X	Y	Z
1	O	8	-2.61624	-0.00479	-0.01085

2	H	1	-2.93071	-0.7917	0.44024
3	O	8	-2.428	-2.49346	-0.01234
4	O	8	-0.57926	-3.50702	-0.00825
5	O	8	3.64863	-1.06917	0.00492
6	O	8	3.64652	1.07441	0.00663
7	O	8	-0.63158	3.53099	-0.00274
8	O	8	-2.42584	2.49292	-0.00834
9	N	7	-1.1905	-2.47807	-0.00905
10	N	7	3.02878	0.00201	0.00413
11	N	7	-1.22904	2.494	-0.00516
12	C	6	-1.18629	0.00746	-0.00704
13	C	6	-0.47139	-1.19598	-0.00611
14	C	6	0.88529	-1.17912	-0.0025
15	H	1	1.42827	-2.10111	-0.00179
16	C	6	1.55879	5.7E-4	2.36E-4
17	C	6	0.86075	1.21768	-6.38E-4
18	H	1	1.39842	2.14277	0.00153
19	C	6	-0.4929	1.2216	-0.00423

Table S7. Coordinates of TNP molecule obtained from DFT calculations.

Center Number	Atom	Atomic Number	Coordinates (Angstroms)		
			X	Y	Z
1	C	6	0.70387	-0.99063	0.0000
2	C	6	1.16931	0.26183	0.0000
3	C	6	-0.82656	-0.88821	0.0000
4	N	7	0.0000	1.14482	0.0000
5	N	7	-1.18508	0.37023	0.0000
6	H	1	1.28495	-1.8891	0.0000
7	H	1	2.19641	0.56175	0.0000
8	H	1	-1.4994	-1.72019	0.0000
9	H	1	0.03393	2.14425	0.0000

Table S8. Coordinates of **CL** molecule obtained from DFT calculations.

Center Number	Atom	Atomic Number	Coordinates (Angstroms)		
			X	Y	Z
1	O	8	1.47495	-1.81019	0.44238
2	O	8	-0.01136	-3.21125	-0.25798
3	O	8	-4.62647	-1.90994	-0.40632
4	O	8	-5.11569	-0.06772	0.63834
5	O	8	-1.91194	3.50939	-0.43308
6	O	8	0.00877	3.15773	0.49141
7	O	8	1.00425	0.76493	-0.33458
8	N	7	0.35075	-2.06494	0.02518
9	N	7	-4.31866	-0.82056	0.07968

10	N	7	-1.04309	2.75795	4.02E-4
11	C	6	-1.29728	1.3164	-0.03616
12	C	6	-0.1824	0.39425	-0.13881
13	C	6	-0.62495	-0.98539	-0.06858
14	C	6	-1.94554	-1.37237	-0.05436
15	H	1	-2.17707	-2.29308	-0.08077
16	C	6	-2.9309	-0.40419	-0.00117
17	C	6	-2.62115	0.94518	0.02139
18	H	1	-3.3081	1.59916	0.07432
19	N	7	4.31495	0.99905	-0.19125
20	N	7	3.54799	-0.10107	-0.14419
21	C	6	5.58027	0.6538	0.03147
22	H	1	6.3237	1.24522	0.05996
23	C	6	5.62638	-0.71053	0.21624
24	H	1	6.39675	-1.23973	0.38688
25	C	6	4.32566	-1.14951	0.10199
26	H	1	4.03507	-2.05027	0.18501
27	H	1	2.67782	-0.02573	-0.21453
28	H	1	3.92752	1.78193	-0.35298

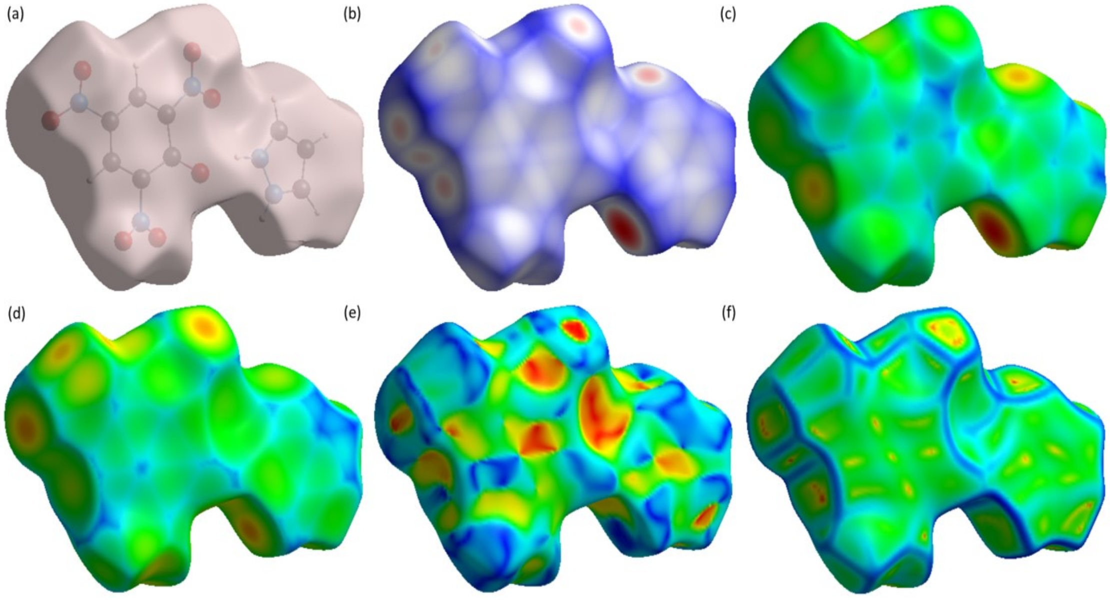

Fig. S9. Hirshfeld surface of **CL** mapped with (a) none, (b) d_{norm}, (c) d_i, (d) d_e, (e) shape index and (f) Curvedness.

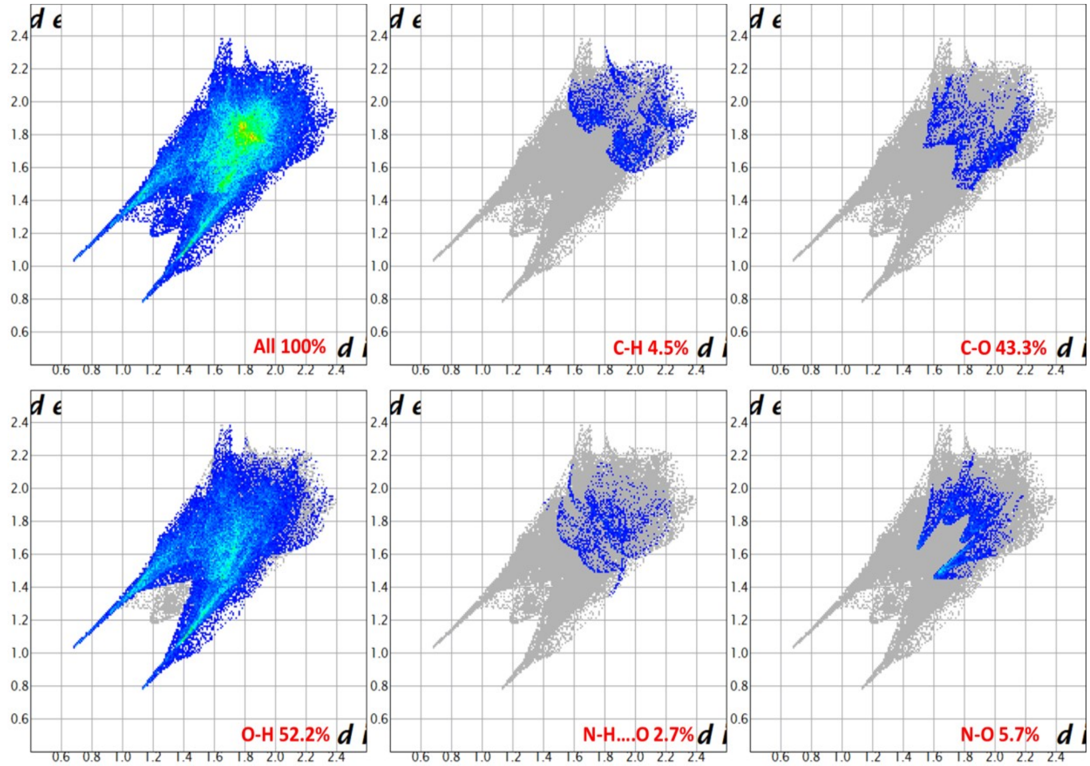

Fig. S10. 2D fingerprint plots of **CL** (charge transfer complex).

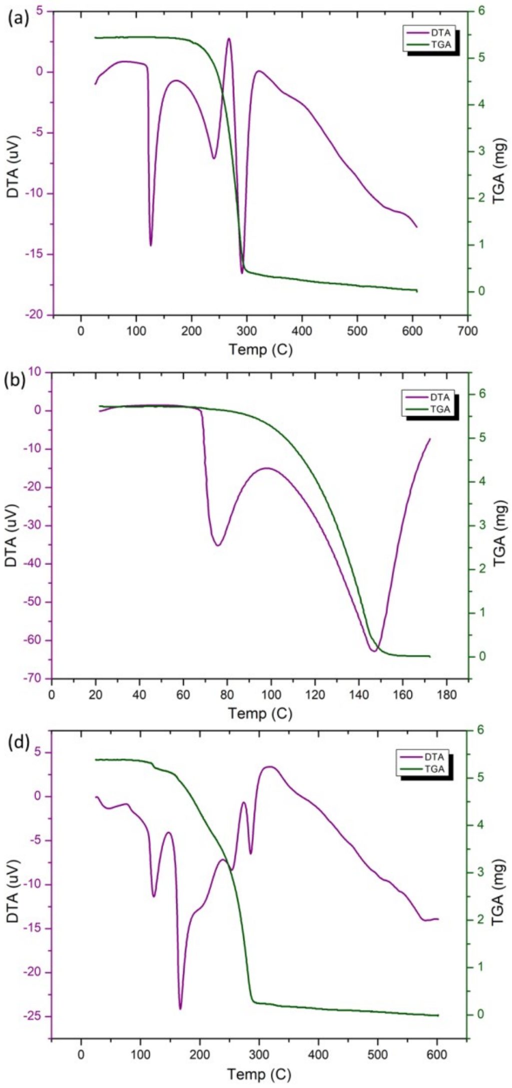

Fig. S11. TGA–DTA curves for (a) TNP, (b) PYZ, and (c) **CL** (charge transfer complex).

References

1. L. Miyan, S. Qamar, and A. Ahmad, *J. Mol. Liq.,* 2017, **225**, 713-722.

2.. L.J. Bellamy, Chapman and Hall, London, The infrared spectra of complex molecules 1975.

3. M.R. Islam, S. Shakya, A. Selim, M.S. Alam, M. Ali, *J. Chem. Eng. Data*, 2019, **64**, 4169-4180.